Article

Lighting up Live Cells with Smart Genetically Encoded Fluorescence Probes from GMars Family

Sheng Wang, Yao Shuai, chaoying sun, Boxin Xue, Yingping Hou, Xiaodong Su, and Yujie Sun

ACS Sens., **Just Accepted Manuscript** • DOI: 10.1021/acssensors.8b00449 • Publication Date (Web): 15 Oct 2018

Lighting up Live Cells with Smart Genetically Encoded Fluorescence Probes from GMars Family

Sheng Wang[1, 2, 4], Yao Shuai[1, 3, 4], Chaoying Sun[1, 2, 4], Boxin Xue[1, 2], Yingping Hou[1, 2], Xiaodong Su[1,3] and Yujie Sun*[,1,2,]

[1] *Biomedical pioneering innovation center (BIOPIC), School of Life Sciences, Peking University, Beijing 100871, China*

[2]*State Key Laboratory of Membrane Biology, Peking University, Beijing 100871, China*

[3] *State Key Laboratory of Protein and Plant Gene Research, Peking University, Beijing 100871, China*

[4] *Contributed equally to this work*

*Corresponding Author, sun_yujie@pku.edu.cn

ABSTRACT

As a special kind of delicate light-controllable genetically encoded optical device, reversibly photoswitchable fluorescent proteins (RSFPs) have been widely applied in many fields, especially various kinds of advanced nanoscopy approaches in recent years. However, there are still necessities for exploring novel RSFPs with specific biochemical or photophysical properties not only for bioimaging or biosensing applications but also for fluorescent protein (FP) mechanisms study and further knowledge-based molecular sensors or optical actuators' rational design and evolution. Besides previously reported GMars-Q and GMars-T variants, herein, we reported the development and applications of other RSFPs from GMars family, especially some featured RSFPs with desired optical properties. In the current work, in-vitro FP purification, spectra measurements and live-cell RESOLFT nanoscopy approaches were applied to characterize the basic properties and test the imaging performances of the selected RSFPs. As demonstrated, GMars variants such as GMars-A, GMars-G, or remarkable photofatigue resistant GMars-L were found with beneficial properties to be capable of parallelized RESOLFT nanoscopy in living cells while other featured GMars variants such as dark GMars-P may be a good candidate for further biosensor or actuator design and applications.

KEYWORDS: *fluorescent protein, reversibly photoswitchable, GMars, live-cell imaging, nanoscopy, RESOLFT, fluorescent probe, biosensor*

As a special kind of “smart” genetically encoded fluorescent probe with fluorescence emission that can be repeatedly and reversibly fine-tuned (*e.g.* on/off) by external lights of different wavelengths (*e.g.* 405nm, 488nm, 561nm, *et.al*),[1-3] reversibly photoswitchable fluorescent proteins (RSFPs) have been widely applied in many fields such as optical data storage,[4] measurements of photochromic fluorescence resonance energy transfer (pcFRET)[5-6] and super-resolution fluorescence imaging based on reversible saturable optical fluorescence transitions (RESOLFT)[7-8] or photochromic stochastic optical fluctuation imaging (pcSOFI).[9-12]

In an effort to develop and optimize RSFPs with special characteristics for various applications, starting with template mMaple3,[13] a green-to-red photoconvertible fluorescent protein which demonstrated good performance for PALM imaging, we have generated a series of reversibly photoswitchable fluorescent proteins (GMars family) which differ from one to another with only one amino acid substitution. We previously demonstrated two bright mutants from GMars family named GMars-Q [mMaple3 (H71Q, M168A)][14] and GMars-T [mMaple3 (H71T, M168A)][15] which displayed special characteristics for long-term parallelized RESOLFT imaging or multimodal subdiffraction structural and functional fluorescence imaging in live cells. Here in this extension work, in order to display the full map of GMars family variants, we first reported and compared the general photophysical properties of all GMars variants as the basis for sophisticated selection, development and applications of RSFPs from mMaple3-derived GMars family. We then mainly demonstrated typical applications of a featured variant from GMars family named GMars-L [mMaple3 (H71L, M168A)] with improved photostability for low light RESOLFT super-resolution imaging in live cells. Finally, we discussed further directions of potential evolution, optimization and applications of genetically encoded fluorescent probes from GMars family specifically for bioimaging and biosensing in live cells at subdiffraction length scale. Thus, this work not only greatly expands the current existing green RSFPs toolbox mainly evolved from

Hydrozoan-derived GFP (*e.g.* rsGreens family)[16-22] and Anthozoan-derived Dronpa[23-28] or mEosFP (*e.g.* mGeos family),[8, 12, 29-30] but also laid the foundation for further comparable analysis, rational evolution and smart application of RSFPs with desired fluorescence properties.

RESULTS AND DISCUSSION

Generation of GMars family proteins based on mMaple3.

We generated reversibly photoswitchable fluorescent proteins using a green-to-red photoconvertible fluorescent protein mMaple3 as template.[13] we analyzed the sequence of mMaple3 to another coral-derived fluorescent protein (FP) mEosFP (Figure S1) and found that most of the amino acids showed high similarity (78%). It was previously reported that changing the bulky residue of M159 to smaller residues such as Ala could induce efficient on-off photochromism of mEosFP,[31] thus In order to induce efficient on-off photochromism of mMaple3, we made a comparable mutation M168A to mMaple3. This new mutant [mMaple3 (M168A)] not only can be photoconverted from green to red form after violet light illumination as mMaple3, but also gain a new characteristic that is reversibly photoswitchable in both its green and red form just like previously reported IrisFP,[32] NijiFP[31] or pcDronpa.[25] We named this new variant Mars for mMaple3 with reversibly switchable characteristics. We next made saturation mutations to the first amino acid of Mars chromophore tripeptide HYG as conducted in previous mGeos work[30] to inhibit its photoconversion from the green to the red form and finally produced a new series of green reversibly photoswitchable fluorescent proteins (Figure S2), GMars (green form Mars) family.

Characterization of GMars family proteins.

Except from GMars-P and GMars-W, screening of GMars family identified 17 bright fluorescent GMars variants after prokaryotic expression and in-vitro

purification (Figure 1a, b). All the fluorescent GMars variants exhibited similar excitation and emission spectra (Ex_{max}=468-474nm, Em_{max}=495-499nm) (Figure 1c), with pK_a range between 4.5~6.5 (Table S-1). Of particular interest, in sharp contrast to almost transparent GMars-W or other bright emerald GMars variants protein solution (1mg/mL) under daylight, solution of GMars-P exhibited light yellow color (Figure S3a). Although no notable specific excitation and emission spectral of GMars-P could be detected both in-vitro and in live cell, GMars-P variant exhibited pronounced specific absorption spectra (Figure S3b, Ab_{max}=474nm), indicating that chromophore (PYG) was readily formed in GMars-P variant while the absorbed energy might dissipate mainly through other non-radiative pathways.[33] Other two interesting variants are GMars-R and GMars-Y, although protein solution of GMars-R displayed extremely weak fluorescence and protein solution of GMars-Y displayed greenish fluorescence under blue light excitation, the specific absorption and fluorescence (excitation/emission) could not be detected in live mammalian cells (*e.g.* HeLa cells, U2OS cells), suggesting that chromophore formation, maturation, and/or protein folding might be severely hindered in live mammalian cell conditions. All the GMars variants are monomers in solution with molecular weight around 27 kDa (Figure S4). Oligomeric states of some GMars variants were also tested directly in living HeLa cells (Table S-2). As a special kind of genetically encoded fluorescent probe mostly applied in protein tagging, imaging and biosensing in live cells, we then directly characterized the general characteristics of all fluorescent GMars variants in live mammalian cells.

As the equilibrium state of all fluorescent GMars variants is bright (on), we directly measured the in-cell brightness of various GMars variants in live HeLa cells relative to previously reported GMars-Q. The measurement indicated that variants such as GMars-T displayed the highest ensemble brightness while GMars-I displayed the lowest ensemble brightness in live cells (Figure S5).

We then measured the photoswitching characteristics of all fluorescent

GMars variants under the same illumination conditions in live HeLa cells. Multiple photoswitching cycles were generated by alternating irradiation with 488 nm and 405 nm light and recorded in living cells expressing individual GMars variant (Figure 1d, Figure S6). The off-switching time constant (τ) of individual GMars variant was determined by fitting off-switching curve of each GMars variant respectively (Figure S7,Table S-1). The data indicated that GMars-M is the slowest photoswitching variant ($\tau \approx$7500 ms) with the highest residual fluorescence (~14%) while GMars-V is the fastest photoswitching variant ($\tau \approx$250 ms) with the lowest residual fluorescence (~0.5%) (Table S-1). However, there is no strict correlation between off-switching time constants and residual fluorescence (Figure S8). Additionally, we also measured thermo stability of various GMars variants in live cells. The data indicated that different GMars variants have different thermo stabilities (Figure S9).

We next characterized photofatigue resistant of all fluorescent GMars variants over 2000 switching cycles at switching light conditions (405nm, 0.1kW/cm^2, 2ms, 488nm, 1kW/cm^2, 24ms) typically used for parallelized RESOLFT imaging.[34] As indicated in Figure S10, GMars-V, the fastest photoswitching variant, showed the highest photofatigue resistant while other slow photoswitching GMars variants such as GMars-M($\tau \approx$ 7500 ms), GMars-C($\tau \approx$3200 ms), GMars-S ($\tau \approx$2800 ms) or GMars-D($\tau \approx$2100 ms) showed low photofatigue resistant. Under such photoswitching conditions, most GMars variants such as GMars-L($\tau \approx$650 ms),GMars-I($\tau \approx$1000 ms) or previously reported GMars-T($\tau \approx$ 400 ms)[15] displayed approximately monophasic photobleaching process while a few GMars variants such as GMars-D, GMars-N($\tau \approx$1300 ms) or previously reported GMars-Q($\tau \approx$800 ms)[14] displayed pronounced biphasic photobleaching process in live cells. In general, although the correlations between photoswitching kinetics and photofatigue resistant are in accordance with previous report that photostability of RSFPs are mainly determined by their photoswitching kinetics rather than the intrinsic resistant to photobleaching,[19] there are two exceptional GMars

variants, GMars-L and GMars-I which showed extremely high photofatigue resistant even taking photoswitching kinetics into consideration. However, GMars-I displayed low ensemble brightness which precluded its further applications as an optimal fluorescent probe in live mammalian cells, we then mainly focused on another selected GMars variant, GMars-L which displayed moderate brightness, relatively fast photoswitching kinetics, low residual fluorescence (~1%) as previously reported GMars variants (Figure 1e), but remarkably higher photofatigue resistant which is different from biphasic photobleaching found in GMars-Q. The photofatigue resistant of GMars-L is significantly higher than that of GMars-T, GMars-Q or rsEGFP(N205S) ($\tau \approx$ 800 ms)[34] (Figure 1f), and even comparable to that of previously reported highly photofatigue resistant RSFP, rsEGFP2 ($\tau \approx$300 ms)[18] which switched ~2.2 folds faster than GMars-L.

Subdiffraction live-cell imaging with selected GMars variants.

Except from GMars-L and previously reported GMars-Q, we found other two bright efficient photoswitching GMars variants, GMars-A ($\tau \approx$800 ms) and GMars-G ($\tau \approx$850 ms) with switching kinetics much similar as rsEGFP(N205S) (Figure S7, Figure S11), but with ~2.7-fold or ~1.3-fold lower residual fluorescence than rsEGFP(N205S) respectively (Figure S7,Table S-1). As rsEGFP(N205S) has already been successfully applied in parallelized RESOLFT microscopy,[34] we then explored the super-resolution imaging performances of similar photoswitching GMars-A, GMars-G and GMars-L in various subcellular structures and organelles using a commercialized parallelized RESOLFT microscope. All the results indicated significantly improved spatial resolution (Figure 2a-i, Figure S12). Specifically for GMars-L, the effective spatial resolution was quantified by measuring intensity profiles of intracellular filamentous structures such as EB3-GMars-L labeled microtubules. The full width at half maximum (FWHM) indicates a resolution of ~85 nm under relative low turn-off laser power (~1kW/cm^2) (Figure 2j-q). We also tested the

imaging performance of the fastest photoswitching variant GMars-V (Figure S13). Although GMars-V displayed the lowest residual fluorescence, the fastest photoswitching kinetics and the highest photofatigue resistant, the individual reconstructed parallelized RESOLFT frame of live cell has comparable low signal-to-background (S/B) ratio mainly because of less photons emitted per fastest switching cycle of GMars-V. So, for live-cell RESOLFT nanoscopy imaging, there exists such a trade-off between switching kinetics which is directly related to achievable temporal resolution and emitted photons which is directly related to S/B ratio of each reconstructed RESOLFT frame.[34]

As GMars-L displayed remarkable photofatigue resistant among all GMars variants, we then tested its ability for time-lapse super-resolution imaging on the same commercialized parallelized RESOLFT microscope. As an example, tagging GMars-L to endoplasmic reticulum (ER) with KDEL sequence enabled continuous live-cell imaging and tracking of ER network remodeling at high spatiotemporal resolution (~3s/frame) (Figure 3). Although the long-term super-resolution imaging capability of GMars-L is comparable to that of previously reported GMars-Q, the photobleaching patterns of the two GMars variants are dramatically different. In sharp contrast to GMars-Q which displayed pronounced biphasic photobleaching process, GMars-L displayed monophasic photobleaching under parallelized RESOLFT microscopy in live cells similar as rsEGFP(N205S), but with dramatically delayed process (Figure S14a-d). Thus, in addition to GMars-Q, GMars-L could be another featured highly photofatigue resistant RSFP from GMars family cable of long-term parallelized RESOLFT nanoscopy. However, there is still space to further improve the ensemble brightness (*e.g.* folding or maturation efficiency) of GMars-L by incorporating directed beneficial mutations as previous efforts.[19] It is also interesting to expect further study could shed light on the mechanisms related to the highly photofatigue resistant of GMars-L in live cells.

During past decade, the development and applications of various RSFPs

have greatly promoted such special light-tunable genetically encoded optical highlighters as indispensible “smart” probes for structural bioimaging and functional biosensing beyond diffraction limit.[35-36] For example, super-resolution optical imaging mainly based on target-coordinated photoswitching (RESOLFT) of RSFPs at ensemble level or stochastic photoswitching of RSFPs at single pixel level (pcSOFI) has enabled unprecedented visual angle of dynamic subcellular structures at subdiffraction length scale in live cells. In addition, molecular biosensors or optical actuators based on RSFPs has enabled detection and super-resolution visualization of kinases’ activities[37] or protein-protein interactions (PPIs),[38-39] viscosity biosensing[40] or even optogenetic control of biomolecules in live cells[41] which are unimaginable before. Although many RSFPs with special optical and biophysical properties have already been developed in recent years, there is still space and necessity to explore and optimize RSFPs with special characteristics (e.g. highly photofatigue resistant RSFPs) not only for bioimaging or biosensing applications but also for FP mechanisms study. More importantly, RSFPs are really complicate devices, although after many years of FP study, there are still surprising discoveries especially to the “dark side” of FP[42-43] and people are still lacking in sufficient knowledge to rational design specific RSFP with desired fluorescence properties.[44] So our current study not only greatly expand the RSFP toolbox and nicely complement to the existing developed RSFPs from Hydrozoan-derived EGFP (*e.g.* rsGreens family) or especially also Anthozoan-derived mEosFP (*e.g.* mGeos family), but also provide valuable research samples with diverse featured properties for further comparable FP structural analysis[45-46] and photophysical mechanisms study. Such study[47-48] will undoubtedly benefit further probes or biosensors rational design and application based on RSFPs.[49-50]

As mMaple3 shares high sequence and origin similarities with another photoconvertible fluorescent protein mEosFP,[29] such similarities also leads to direct biochemical and photophysical properties comparison which can be

even traced back to their parental ancestor FPs between mMaple and mEos2.[51] It is very interesting to note that mMaple3-derived RSFPs from GMars family also share some similarities with mEos2-derived RSFPs from mGeos family.[30] For example, RSFP variants such as mGeos-C, mGeos-S and mGeos-M or corresponding GMars-C, GMars-S and GMars-M exhibited relatively slow switching kinetics while mGeos-A, mGeos-L, mGeos-Q, mGeos-T and mGeos-V or corresponding GMars-A, GMars-L, GMars-Q, GMars-T and GMars-V exhibited relatively fast switching kinetics among mGeos and GMars family respectively. Variants such as mGeos-I and mGeos-V or corresponding GMars-I and GMars-V stand out for their high photofatigue resistant. However, such correspondence relationship is not always when taking relative switching kinetics of mGeos-F and GMars-F or photofatigue resistant of mGeos-L and GMars-L into consideration. Thus, further study including protein structure determination[32, 52] and comparable structure analysis are still awaited for further characterizing structure-function relationship[53 54]of both mGeos and GMars family proteins, which might in-turn, benefit “superb hybrid” RSFP design and applications (*e.g.* integration of desired properties from both mGeos and GMars family through rational design and selection).

As RSFPs from GMars family displayed various switching kinetics, having such broad “color” palette, In addition to single-channel RESOLFT nanoscopy, dual-channel RESOLFT nanoscopy might be readily enabled by discerning different switching kinetics (τ) of elaborately selected GMars variants rather than their similar spectra.[55] For example, in previous report, Dronpa (M159T) and rsEGFP(N205S) have been successfully applied in dual-channel point scanning live-cell RESOLFT nanoscopy(τ-RESOLFT). Thus, it is possible to realize such “multicolor” imaging modal with GMars-V whose photoswitching kinetics are quite similar as the previously reported the fastest photoswitching Dronpa(M159T) (Figure S15) paired with GMars variants such as GMars-Q, GMars-A or GMars-G whose photoswitching kinetics are quite similar as

rsEGFP(N205S). Such similar smart concept has also been applied in dual-label pcSOFI nanoscopy recently.[56]

Except from bioimaging as genetically encoded fluorescent probes, there are still spaces to further evolve some featured RSFPs from GMars family as molecular biosensors or optical actuators. For example, dark GMars-P with extremely low quantum yield (QY) could be a good candidate further optimized as genetically encoded non-fluorescent photochromic acceptor for pcFRET measurement similar as previously reported Phanta[6] or molecular quencher for proteases or kinases activity biosensing and imaging similar as previously reported sREACh,[57] ShadowG,[58] ShadowY[59] or ultramarine[60] applied in FLIM-FRET measurement. GMars-V might also be a good candidate for high speed reversible data optical storage due to its fastest switching kinetics and highest photofatigue resistant among all GMars variants. GMars-E might be readily applied in repeated and reversible fluorescence recovery after photobleaching (FRAP) or fluorescence loss in photobleaching (FLIP) measurement for protein trafficking and mobility study due to its relatively slow photoswitching kinetics ($\tau \approx 2000$ ms) and high imaging contrast or low residual fluorescence (2%) in live cells.[61] Another valuable application of RSFPs from GMars family is that such extremely similar RSFP variants (sequence similarity or homology) could be readily adapted for detecting and imaging PPIs at subdiffraction length scale in live cells based on bimolecular fluorescence complementation (BiFC).[15, 62] Similar as previously reported GMars-T, BiFC assays might also be conveniently established among most GMars variants such as GMars-V, GMars-A ,GMars-G and GMars-Q at the same conserved splitting site between 173K and 174G (Figure S16, Figure S17, Figure S18). More importantly, since all the splitted GMars variants share exactly the same C-terminal fragment while with only one amino acid difference in their N-terminal fragments, similar as previously established multicolor BiFC derived from GFP variants,[63] cross-complementation among splitted GMars variants between different N-terminal fragments and the same

C-terminal fragment enable “multicolor” BiFC which could be easily applied to detect and compare the subcellular distributions of several protein complexes in the same cell or analyze the competition between mutually exclusive interaction partners for binding to a common partner at subdiffraction length scale.

Besides the applications in live mammalian cells, it should also be very interesting and meaningful to explore the potential applications of GMars family proteins or their derived molecular biosensors or optical actuators in prokaryotic cells,[20] plant cells,[64] multicellular organs[65-66] or even possible whole-animals.[67]

Except from some featured GMars variants discussed above in the current work, on one hand, further efforts are still awaited to explore more potentials or new properties (*e.g.* “blinking”)[68-69] on RSFPs from GMars family for advanced bioimaging and smart biosensing applications; on the other hand, RSFPs structure determination combined with comparable structure analysis and molecular dynamics (MD) simulation are urgently needed to elucidate FP structure-function relationships or mechanisms for further improvement the performances of existing RSFPs[70] or rational evolution of novel RSFPs with desired properties. Also challenges exists,[71] it would still be very exciting and also worth expecting that further mechanisms study, knowledge-based rational design and elaborate evolution will turn GMars family proteins into a new set of powerful genetically encoded optical imaging probes, molecular biosensors or even actuators in various smart applications. Such efforts will undoubtedly make these precious “crazy diamonds” shine on.[72]

CONCLUSIONS

In this work, we have developed a new series of green RSFPs (GMars family proteins) with various biochemical and photophysical properties. Specifically, we demonstrated live-cell super-resolution RESOLFT imaging with GMars-L

which displayed remarkable high photofatigue resistant which is different from previously reported GMars-Q. We also reported and compared the general photophysical properties of all GMars variants and discussed further directions of potential evolution, optimization and applications of genetically encoded fluorescent probes from GMars family specifically for bioimaging and biosensing in live cells at subdiffraction length scale. Although there is still space to further optimize or improve the desired properties of RSFPs from GMars family, the current work not only greatly expanded RSFP toolbox with many featured properties, but also laid the foundation for further sophisticated selection, development and applications of RSFPs as a new set of powerful bioimaging and biosensing probes from mMaple3-derived GMars family.

MATERIALS AND METHODS

Plasmid Design and Construction.

We constructed pGMars-X-N1and pGMars-X-C1 vectors by inserting GMars-X cDNA sequences into pEGFP-N1 (Clontech) and pEGFP-C1 (Clontech) vectors using BamH Ⅰ/Not Ⅰ and Nhe Ⅰ/HindⅢ sites respectively to replace EGFP gene sequences, where X stands for other 19 naturally occurring amino acids except histidine (H). Similarly, prsCherryRev1.4-N1 and prsCherryRev1.4-C1 vectors were generated accordingly. To generate GalT-7-GMars-G vector, GalT-7 sequences were tagged to the N-terminal of GMars-G sequences and subcloned into pcDNA3.1 (+) vector with BamH Ⅰ /EcoR Ⅰ sites. To generate ER-GMars-G or ER-GMars-L vectors, ER targeting sequences KDEL were tagged to the C-terminal of GMars-G or GMars-L sequences and subcloned into pcDNA3.1 (+) vector with the same BamH Ⅰ /EcoR Ⅰ sites respectively. To generate Lifeact-GMars-G vectors, the cDNA of Lifeact sequences were tagged to the N-terminal cDNA sequences of GMars-G. The fusion cDNA sequences were inserted into pcDNA3.1 (+) vector using BamH Ⅰ /EcoR Ⅰ sites. To generate H2B-GMars-L vector, H2B cDNA

sequences (*Homo sapines*) were inserted into pGMars-L-N1 vector with Nhe Ⅰ /HindⅢ sites. To construct EB3-GMars-L and EB3-GMars-A vectors, the cDNA sequences of EB3 were amplified and inserted into pGMars-L-N1 and pGMars-A-N1 vectors using NheI/HindIII sites respectively. To generate Mito-GMars-L or Mito-rsCherryRev1.4 vectors, mitochondria targeting sequences were tagged to the N-terminal sequences of GMars-L or rsCherryRev1.4 and subcloned into pcDNA3.1 (+) vector with BamH Ⅰ /EcoR Ⅰ sites respectively. To generate Keratin19-GMars-A vector, the full-length Homo sapines Keratin19 cDNAs with Nhe Ⅰ /HindⅢ sites were PCR-amplified and inserted into pGMars-A-N1 vector. To generate Vimentin-GMars-A vector, the full-length of Homo sapines Vimentin cDNAs with Nhe Ⅰ /HindⅢ sites were PCR-amplified and inserted into pGMars-A-N1 vector. For measuring the relative in-cell brightness of individual GMars variant, mCherry-P2A-GMars-X constructs were generated by inserting mCherry-P2A sequences into Nhe Ⅰ / BamH Ⅰ sites and GMars-X sequences into BamH Ⅰ /EcoR Ⅰ sites of pcDNA3.1(+) vector respectively.

Protein Expression and Purification.

GMars-X cDNA sequences were subcloned into pET15b (Novagen, Madison, WI) expression vector and protein expression was conducted in E. *coli* strain BL21 (DE3) after isopropyl β-d-thiogalactoside (IPTG) induction. Then, protein purification was performed using Ni^{2+}-nitrilotriacetate affinity resin (Ni-NTA; Qiagen, Hilden, Germany). Further purification was performed by size-exclusion chromatography.

Measurements of Spectral Properties and p*K*a.

A SpectraMax M5 (Molecular device, USA) Instrument was used to measure GMars-X spectral properties (absorption, excitation, emission). The fluorescence quantum yield (Φ_{Fl}) was determined relative to the reported value of fluorescein (quantum yield = 0.95, molar extinction coefficient = 70,000 M^{-1}

cm^{-1} at 491 nm). The extinction coefficient (ε) was determined using alkali-denatured method described previously.[73] We used glycine-hydrochloric acid buffer (for pH $\leqslant$ 5) or sodium phosphate buffer (for pH $\geqslant$ 6) with different pH values (2~11) to measure p*K*a of GMars protein variants. The p*K*a value was taken as the pH value where the fluorescence emission reached 50% of the maximum.[74]

Cell Culture and Transfection.

DMEM complete medium (Gibco, Eggenstein, Germany) supplemented with 10% fetal bovine serum was used for cell culture. U2OS and HeLa cells were maintained at 37°C and 5% CO_2 in a humidified incubator. Cells transient transfection was performed using Lipofectamine™ 2000 (Invitrogen Carlsbad, CA). For RESOLFT imaging, cells were grown in IMEM (Gibco, Eggenstein, Germany) or DMEM complete medium without phenol red.

Measuring the Relative In-Cell Brightness of RSFPs from GMars family.

For in-cell brightness measurement, we generated mCherry-P2A-GMars-X expression vectors. In such constructs design, live HeLa cells produce mCherry and a GMars variant of interest separately in a 1:1 ratio.[75] Green and red fluorescence in live cells were measured by flow cytometry from three independent measurement and the green/red fluorescence intensity ratio was determined from individual live cell and totally at least 50000 cells were analyzed for each GMars variant. The relative in-cell brightness of individual GMars variant was calculated relative to the ratio of GMars-Q, and then the data were presented as means±SEM values.

Measuring the photoswitching properties of RSFPs.

Photoswitching kinetics of GMars variants were analyzed using an inverted fluorescent microscope (Olympus, IX81). We used 405 nm violet light (25 W/cm^2) to activate RSFPs and 488 nm blue light (50 W/cm^2) to off-switch

RSFPs. The off-switching time constant (τ) was determined by fitting the off-switching curve of each GMars variant.

RESOLFT Nanoscopic Imaging.

RESOLFT experiments were carried out on a commercial parallelized RESOLFT microscope (2-color RESOLFT Parallel, Abberior Instruments, Germany). A 405 nm continuous wave diode laser was used for on-switching; 488 nm and 592nm continuous wave lasers were used for off-switching and fluorescence readout. A 100×, NA 1.45 oil-immersion objective lens (IX83, Olympus) was equipped for imaging. Two independent sCMOS cameras (Hamamatsu, Flash 4.0) were equipped for two-color RESOLFT microscope. Unless specified, RESOLFT images were always taken using 36 nm scanning step (pixel) size and $(360/36)^2$ steps are required for each frame. For GMars-V imaging, a 405 nm continuous wave diode laser was used for on-switching (2 ms, 12 mW measured at the back focal plane of the objective, corresponding to 0.1 kW/cm^2); a 488 nm continuous wave laser was used for off-switching (10 ms, 50 mW measured at the back focal plane of the objective, corresponding to 1 kW/cm^2); and fluorescence readout (4 ms, 50 mW measured at the back focal plane of the objective). For rsEGFP(N205S) or GMars-A, GMars-G, and GMars-L imaging, a 405 nm continuous wave diode laser was used for on-switching (2 ms); a 488 nm continuous wave laser was used for off-switching (20 ms); and fluorescence readout (4 ms). For rsCherryRev1.4 imaging,[76] a 405 nm continuous wave diode laser was used for on-switching (2 ms); a 592 nm continuous wave laser was used for off-switching (80 ms) and fluorescence readout (10 ms).

ASSOCIATED CONTENT

SUPPORTING INFORMATION

Additional information as noted in text. This material is available free of charge via the Internet at http://pubs.acs.org.

Experimental details and data (PDF)

AUTHOR INFORMATION

Corresponding Author

*E-mail: sun_yujie@pku.edu.cn. Tel: 86-13051402289.

Author Contributions

S.W. and Y.S. designed the project. S.W. performed protein mutation and applications. S.W., Y.S., C.S., B.X., Y.H. performed protein characterization. S.W. X.S. and Y.S. wrote and revised the manuscript.

Notes

The authors declare no competing financial interest.

ACKNOWLEDGEMENTS

We thank Professor X.W. Zhuang (Department of Chemistry and Chemical Biology, Harvard University) for providing mMaple3 plasmid. This work is supported by grants from the National Key R&D Program of China, No. 2017YFA0505300, and the National Science Foundation of China 21390412 and 31327901 for Y.S.

FIGURES AND LEGENDS

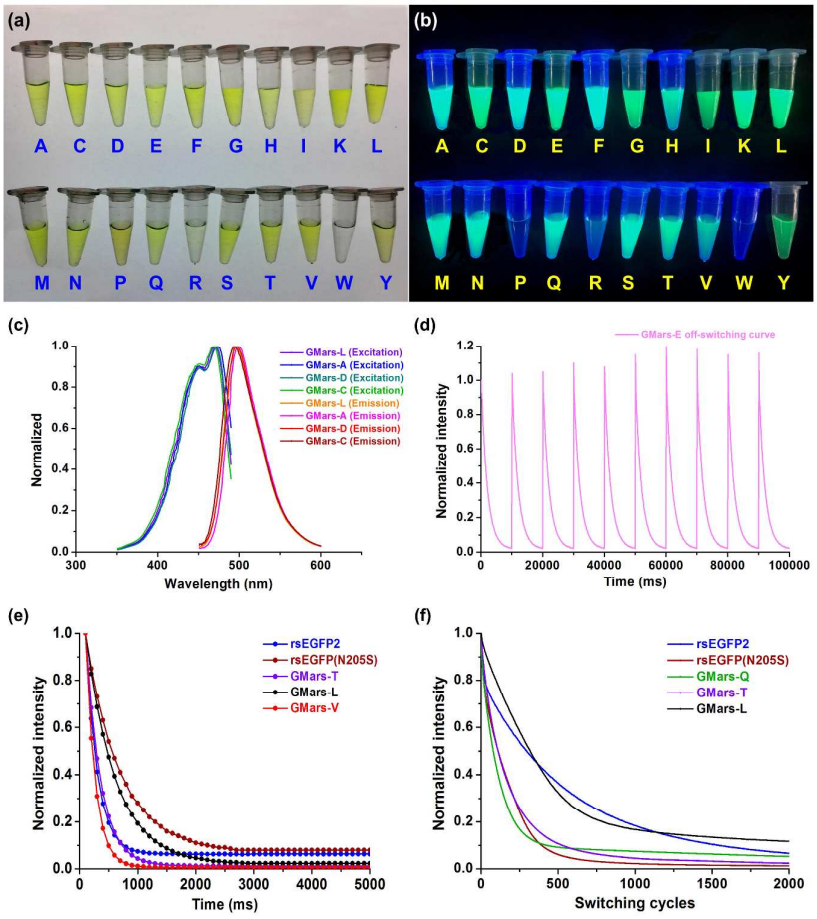

Figure 1 Characterization of GMars variants.

(a) Mars and GMars variants protein solution (1mg/mL) image under daylight. The individual letter below represents the first amino acid substitution to the chromophore tripeptide **H**YG of mMaple3. (b) Corresponding fluorescence image of Mars and GMars variants protein solution under blue light excitation. (c) Excitation and emission spectra of selected 4 GMars variants in its equilibrium state at pH7.5. (d) 10 consecutive normalized off-switching curves of GMars-E in live cells by alternating irradiation with 405 nm light (25 W/cm^2, 100 ms) and 488 nm (50 W/cm^2, 10000 ms). (e) Single ensemble off-switching curves of GMars-T, GMars-L, GMars-V, rsEGFP2 and rsEGFP(N205S) in live cells by alternating irradiation with 488 nm (50 W/cm^2, 5000 ms) and 405 nm light (25 W/cm^2, 100 ms). (f) Switching fatigue of GMars-Q, GMars-T, GMars-L, rsEGFP2 and rsEGFP(N205S) in live cells by alternating irradiation with 405 nm (0.1 kW/cm^2, 2 ms) and 488 nm (1 kW/cm^2, 24 ms) light. Illumination times were chosen so that the fluorescence was fully switched to the minimum or maximum, respectively, in each cycle. Data were presented as averaged data from three independent experiments.

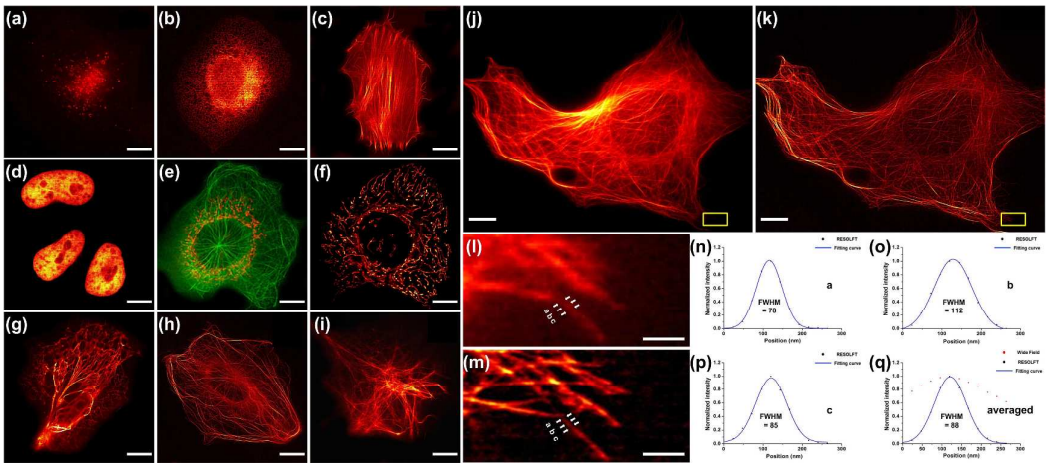

Figure 2 Expression and characterization of various functional selected GMars variants fusion proteins in live mammalian cells by a parallelized RESOLFT microscope.

(a-i) Expression of various GMars variants fusion proteins in live mammalian cells; (a) GalT-7-GMars-G (targeting to Golgi apparatus) in HeLa cell; (b) GMars-G-KDEL (targeting to ER) in HeLa cell; (c) Lifeact-GMars-G (targeting to actin filaments) in HeLa cell; (d) H2B-GMars-L in HeLa cell; (e) EB3-GMars-L (green, targeting to microtubules) and Mito-rsCherryRev1.4 (red, targeting to mitochondria) in U2OS cell; (f) Mito-GMars-L in U2OS cell; (g) Keratin19-GMars-A (targeting to intermediate filaments) in HeLa cell; (h) EB3-GMars-A in U2OS cell; (i) Vimentin-GMars-A (targeting to intermediate filaments) in HeLa cell. (j-q) characterization of the spatial resolution of GMars-L by a cellular filamentous structure; (j) conventional wide-field image of U2OS cell expressing EB3-GMars-L;(k) RESOLFT image of (j); (l) magnified image of the boxed area of (j); (m) magnified image of the box area of (k); (n-p) intensity profiles measured of arrowed a, b, c regions respectively in (m); (q) averaged intensity profile of (n-p). Scale bar: 10 μm in (a-k); 1 μm in (l, m). In Figure 2a-i, 36 nm scanning step (pixel) size was used for RESOLFT image reconstruction. In Figure 2k, 24nm scanning step (pixel) size was used for RESOFLT image reconstruction and resolution quantification.

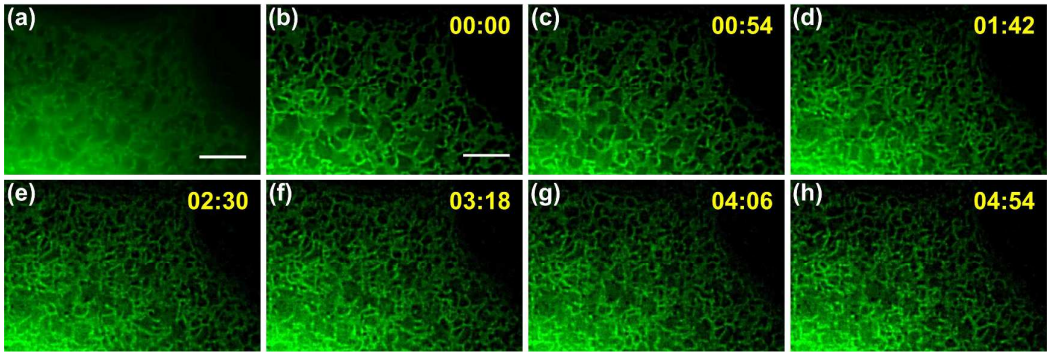

Figure 3 Continuous time-lapse imaging with parallelized RESOLFT.

(a) Conventional wide-field image and (b-h) selected RESOLFT images of ER network dynamics captured in a living HeLa cell expressing GMars-L-KDEL fusion protein from a 50-frame RESOLFT movie, the images are displayed using linear intensity scale without adjusting γ factor. All the RESOLFT images were taken using 36 nm scanning step (pixel) size and $(360/36)^2$ steps were required for one RESOLFT frame. Each RESOLFT image was taken within 3 s. Scale bar: 5μm.

REFERENCES

1. Zhou, X. X.; Lin, M. Z., Photoswitchable fluorescent proteins: ten years of colorful chemistry and exciting applications. *Curr Opin Chem Biol* **2013,** *17* (4), 682-690.

2. Rodriguez, E. A.; Campbell, R. E.; Lin, J. Y.; Lin, M. Z.; Miyawaki, A.; Palmer, A. E.; Shu, X.; Zhang, J.; Tsien, R. Y., The Growing and Glowing Toolbox of Fluorescent and Photoactive Proteins. *Trends Biochem Sci* **2017,** *42* (2), 111-129.

3. Shcherbakova, D. M.; Sengupta, P.; Lippincott-Schwartz, J.; Verkhusha, V. V., Photocontrollable fluorescent proteins for superresolution imaging. *Annu Rev Biophys* **2014,** *43*, 303-329.

4. Adam, V.; Mizuno, H.; Grichine, A.; Hotta, J.; Yamagata, Y.; Moeyaert, B.; Nienhaus, G. U.; Miyawaki, A.; Bourgeois, D.; Hofkens, J., Data storage based on photochromic and photoconvertible fluorescent proteins. *J Biotechnol* **2010,** *149* (4), 289-298.

5. Subach, F. V.; Zhang, L.; Gadella, T. W.; Gurskaya, N. G.; Lukyanov, K. A.; Verkhusha, V. V., Red fluorescent protein with reversibly photoswitchable absorbance for photochromic FRET. *Chem Biol* **2010,** *17* (7), 745-755.

6. Don Paul, C.; Kiss, C.; Traore, D. A.; Gong, L.; Wilce, M. C.; Devenish, R. J.; Bradbury, A.; Prescott, M., Phanta: a non-fluorescent photochromic acceptor for pcFRET. *PLoS One* **2013,** *8* (9), e75835.

7. Hofmann, M.; Eggeling, C.; Jakobs, S.; Hell, S. W., Breaking the diffraction barrier in fluorescence microscopy at low light intensities by using reversibly photoswitchable proteins. *Proc. Natl. Acad. Sci. U. S. A.* **2005,** *102* (49), 17565-17569.

8. Zhang, X.; Zhang, M.; Li, D.; He, W.; Peng, J.; Betzig, E.; Xu, P., Highly photostable, reversibly photoswitchable fluorescent protein with high contrast ratio for live-cell superresolution microscopy. *Proc. Natl. Acad. Sci. U. S. A.* **2016,** *113* (37), 10364-10369.

9. Dertinger, T.; Colyer, R.; Iyer, G.; Weiss, S.; Enderlein, J., Fast, background-free, 3D super-resolution optical fluctuation imaging (SOFI). *Proc. Natl. Acad. Sci. U. S. A.* **2009,** *106* (52), 22287-22292.

10. Dertinger, T.; Colyer, R.; Vogel, R.; Heilemann, M.; Sauer, M.; Enderlein, J.;

Weiss, S., Superresolution optical fluctuation imaging (SOFI). *Adv Exp Med Biol* **2012,** *733*, 17-21.

11. Moeyaert, B.; Dedecker, P., PcSOFI as a smart label-based superresolution microscopy technique. *Methods Mol Biol* **2014,** *1148*, 261-276.

12. Zhang, X.; Chen, X.; Zeng, Z.; Zhang, M.; Sun, Y.; Xi, P.; Peng, J.; Xu, P., Development of a reversibly switchable fluorescent protein for super-resolution optical fluctuation imaging (SOFI). *ACS Nano* **2015,** *9* (3), 2659-2667.

13. Wang, S.; Moffitt, J. R.; Dempsey, G. T.; Xie, X. S.; Zhuang, X., Characterization and development of photoactivatable fluorescent proteins for single-molecule-based superresolution imaging. *Proc. Natl. Acad. Sci. U. S. A.* **2014,** *111* (23), 8452-8457.

14. Wang, S.; Chen, X.; Chang, L.; Xue, R.; Duan, H.; Sun, Y., GMars-Q Enables Long-Term Live-Cell Parallelized Reversible Saturable Optical Fluorescence Transitions Nanoscopy. *ACS Nano* **2016,***10 (10),* 9136–9144.

15. Wang, S.; Chen, X.; Chang, L.; Ding, M.; Xue, R.; Duan, H.; Sun, Y., GMars-T Enabling Multimodal Subdiffraction Structural and Functional Fluorescence Imaging in Live Cells. *Anal Chem* **2018,** *90* (11), 6626-6634.

16. Brakemann, T.; Stiel, A. C.; Weber, G.; Andresen, M.; Testa, I.; Grotjohann, T.; Leutenegger, M.; Plessmann, U.; Urlaub, H.; Eggeling, C.; Wahl, M. C.; Hell, S. W.; Jakobs, S., A reversibly photoswitchable GFP-like protein with fluorescence excitation decoupled from switching. *Nat Biotechnol* **2011,** *29* (10), 942-947.

17. Grotjohann, T.; Testa, I.; Leutenegger, M.; Bock, H.; Urban, N. T.; Lavoie-Cardinal, F.; Willig, K. I.; Eggeling, C.; Jakobs, S.; Hell, S. W., Diffraction-unlimited all-optical imaging and writing with a photochromic GFP. *Nature* **2011,** *478* (7368), 204-208.

18. Grotjohann, T.; Testa, I.; Reuss, M.; Brakemann, T.; Eggeling, C.; Hell, S. W.; Jakobs, S., rsEGFP2 enables fast RESOLFT nanoscopy of living cells. *Elife* **2012,** *1*, e00248.

19. Duwé, S.; De Zitter, E.; Gielen, V.; Moeyaert, B.; Vandenberg, W.; Grotjohann, T.; Clays, K.; Jakobs, S.; Van Meervelt, L.; Dedecker, P., Expression-Enhanced Fluorescent Proteins Based on Enhanced Green Fluorescent Protein for Super-resolution Microscopy. *ACS Nano* **2015,** *9* (10), 9528-9541.

20. El Khatib, M.; Martins, A.; Bourgeois, D.; Colletier, J. P.; Adam, V., Rational design of ultrastable and reversibly photoswitchable fluorescent proteins for super-resolution imaging of the bacterial periplasm. *Sci Rep* **2016,** *6*, 18459.

21. Bizzarri, R.; Serresi, M.; Cardarelli, F.; Abbruzzetti, S.; Campanini, B.; Viappiani, C.; Beltram, F., Single amino acid replacement makes Aequorea victoria fluorescent proteins reversibly photoswitchable. *J Am Chem Soc* **2010,** *132* (1), 85-95.

22. Jensen, N. A.; Danzl, J. G.; Willig, K. I.; Lavoie-Cardinal, F.; Brakemann, T.; Hell, S. W.; Jakobs, S., Coordinate-targeted and coordinate-stochastic super-resolution microscopy with the reversibly switchable fluorescent protein Dreiklang. *Chemphyschem* **2014,** *15* (4), 756-762.

23. Stiel, A. C.; Trowitzsch, S.; Weber, G.; Andresen, M.; Eggeling, C.; Hell, S. W.; Jakobs, S.; Wahl, M. C., 1.8 A bright-state structure of the reversibly switchable fluorescent protein Dronpa guides the generation of fast switching variants. *Biochem J* **2007,** *402* (1), 35-42.

24. Brakemann, T.; Weber, G.; Andresen, M.; Groenhof, G.; Stiel, A. C.; Trowitzsch, S.; Eggeling, C.; Grubmuller, H.; Hell, S. W.; Wahl, M. C.; Jakobs, S., Molecular basis of the light-driven switching of the photochromic fluorescent protein Padron. *J Biol Chem* **2010,** *285* (19), 14603-14609.

25. Moeyaert, B.; Nguyen Bich, N.; De Zitter, E.; Rocha, S.; Clays, K.; Mizuno, H.; van Meervelt, L.; Hofkens, J.; Dedecker, P., Green-to-red photoconvertible Dronpa mutant for multimodal super-resolution fluorescence microscopy. *ACS Nano* **2014,** *8* (2), 1664-1673.

26. Rosenbloom, A. B.; Lee, S. H.; To, M.; Lee, A.; Shin, J. Y.; Bustamante, C., Optimized two-color super resolution imaging of Drp1 during mitochondrial fission with a slow-switching Dronpa variant. *Proc. Natl. Acad. Sci. U. S. A.* **2014,** *111* (36), 13093-13098.

27. Tiwari, D. K.; Arai, Y.; Yamanaka, M.; Matsuda, T.; Agetsuma, M.; Nakano, M.; Fujita, K.; Nagai, T., A fast- and positively photoswitchable fluorescent protein for ultralow-laser-power RESOLFT nanoscopy. *Nat Methods* **2015,** *12* (6), 515-518.

28. Wilmann, P. G.; Turcic, K.; Battad, J. M.; Wilce, M. C.; Devenish, R. J.; Prescott, M.; Rossjohn, J., The 1.7 A crystal structure of Dronpa: a photoswitchable green fluorescent protein. *J Mol Biol* **2006,** *364* (2), 213-224.

29. Wiedenmann, J.; Ivanchenko, S.; Oswald, F.; Schmitt, F.; Rocker, C.; Salih, A.; Spindler, K. D.; Nienhaus, G. U., EosFP, a fluorescent marker protein with UV-inducible green-to-red fluorescence conversion. *Proc. Natl. Acad. Sci. U. S. A.* **2004,** *101* (45), 15905-15910.

30. Chang, H.; Zhang, M.; Ji, W.; Chen, J.; Zhang, Y.; Liu, B.; Lu, J.; Zhang, J.; Xu, P.; Xu, T., A unique series of reversibly switchable fluorescent proteins with beneficial properties for various applications. *Proc. Natl. Acad. Sci. U. S. A.* **2012,** *109* (12), 4455-4460.

31. Adam, V.; Moeyaert, B.; David, C. C.; Mizuno, H.; Lelimousin, M.; Dedecker, P.; Ando, R.; Miyawaki, A.; Michiels, J.; Engelborghs, Y.; Hofkens, J., Rational design of photoconvertible and biphotochromic fluorescent proteins for advanced microscopy applications. *Chem Biol* **2011,** *18* (10), 1241-1251.

32. Adam, V.; Lelimousin, M.; Boehme, S.; Desfonds, G.; Nienhaus, K.; Field, M. J.; Wiedenmann, J.; McSweeney, S.; Nienhaus, G. U.; Bourgeois, D., Structural characterization of IrisFP, an optical highlighter undergoing multiple photo-induced transformations. *Proc. Natl. Acad. Sci. U. S. A.* **2008,** *105* (47), 18343-18348.

33. Shu, X.; Shaner, N. C.; Yarbrough, C. A.; Tsien, R. Y.; Remington, S. J., Novel chromophores and buried charges control color in mFruits. *Biochemistry* **2006,** *45* (32), 9639-9647.

34. Chmyrov, A.; Keller, J.; Grotjohann, T.; Ratz, M.; d'Este, E.; Jakobs, S.; Eggeling, C.; Hell, S. W., Nanoscopy with more than 100,000 'doughnuts'. *Nat Methods* **2013,** *10* (8), 737-740.

35. Tiwari, D. K.; Nagai, T., Smart fluorescent proteins: innovation for barrier-free superresolution imaging in living cells. *Dev Growth Differ* **2013,** *55* (4), 491-507.

36. Andresen, M.; Stiel, A. C.; Folling, J.; Wenzel, D.; Schonle, A.; Egner, A.; Eggeling, C.; Hell, S. W.; Jakobs, S., Photoswitchable fluorescent proteins enable monochromatic multilabel imaging and dual color fluorescence nanoscopy. *Nat Biotechnol* **2008,** *26* (9), 1035-1040.

37. Mo, G. C.; Ross, B.; Hertel, F.; Manna, P.; Yang, X.; Greenwald, E.; Booth, C.; Plummer, A. M.; Tenner, B.; Chen, Z.; Wang, Y.; Kennedy, E. J.; Cole, P. A.; Fleming, K. G.; Palmer, A.; Jimenez, R.; Xiao, J.; Dedecker, P.; Zhang, J., Genetically encoded biosensors for visualizing live-cell biochemical activity at

super-resolution. *Nat Methods* **2017,** *14* (4), 427-434.

38. Hertel, F.; Mo, G. C.; Duwé, S.; Dedecker, P.; Zhang, J., RefSOFI for Mapping Nanoscale Organization of Protein-Protein Interactions in Living Cells. *Cell Rep* **2016,** *14* (2), 390-400.

39. Wang, S.; Ding, M.; Chen, X.; Chang, L.; Sun, Y., Development of bimolecular fluorescence complementation using rsEGFP2 for detection and super-resolution imaging of protein-protein interactions in live cells. *Biomed Opt Express* **2017,** *8* (6), 3119-3131.

40. Kao, Y. T.; Zhu, X.; Min, W., Protein-flexibility mediated coupling between photoswitching kinetics and surrounding viscosity of a photochromic fluorescent protein. *Proc. Natl. Acad. Sci. U. S. A.* **2012,** *109* (9), 3220-3225.

41. Zhou, X. X.; Chung, H. K.; Lam, A. J.; Lin, M. Z., Optical control of protein activity by fluorescent protein domains. *Science* **2012,** *338* (6108), 810-814.

42. Nienhaus, K.; Nienhaus, G. U., Photoswitchable Fluorescent Proteins: Do Not Always Look on the Bright Side. *ACS Nano* **2016,** *10(10),* 9104–9108.

43. Duan, C.; Adam, V.; Byrdin, M.; Ridard, J.; Kieffer-Jaquinod, S.; Morlot, C.; Arcizet, D.; Demachy, I.; Bourgeois, D., Structural evidence for a two-regime photobleaching mechanism in a reversibly switchable fluorescent protein. *J Am Chem Soc* **2013,** *135* (42), 15841-15850.

44. Duan, C.; Byrdin, M.; El Khatib, M.; Henry, X.; Adam, V.; Bourgeois, D., Rational design of enhanced photoresistance in a photoswitchable fluorescent protein. *Methods Appl Fluoresc* **2015,** *3* (1), 014004.

45. Duan, C.; Adam, V.; Byrdin, M.; Bourgeois, D., Structural basis of photoswitching in fluorescent proteins. *Methods Mol Biol* **2014,** *1148*, 177-202.

46. Pakhomov, A. A.; Martynov, V. I., GFP family: structural insights into spectral tuning. *Chem Biol* **2008,** *15* (8), 755-764.

47. Bourgeois, D.; Adam, V., Reversible photoswitching in fluorescent proteins: a mechanistic view. *IUBMB Life* **2012,** *64* (6), 482-491.

48. Andresen, M.; Wahl, M. C.; Stiel, A. C.; Grater, F.; Schafer, L. V.; Trowitzsch, S.; Weber, G.; Eggeling, C.; Grubmuller, H.; Hell, S. W.; Jakobs, S., Structure and mechanism of the reversible photoswitch of a fluorescent protein. *Proc. Natl. Acad. Sci. U. S. A.* **2005,** *102* (37), 13070-13074.

49. Berardozzi, R.; Adam, V.; Martins, A.; Bourgeois, D., Arginine 66 Controls Dark-State Formation in Green-to-Red Photoconvertible Fluorescent Proteins.

J Am Chem Soc **2016,** *138* (2), 558-565.

50. Morozov, D.; Groenhof, G., Hydrogen Bond Fluctuations Control Photochromism in a Reversibly Photo-Switchable Fluorescent Protein. *Angew Chem Int Ed Engl* **2016,** *55* (2), 576-578.

51. McEvoy, A. L.; Hoi, H.; Bates, M.; Platonova, E.; Cranfill, P. J.; Baird, M. A.; Davidson, M. W.; Ewers, H.; Liphardt, J.; Campbell, R. E., mMaple: a photoconvertible fluorescent protein for use in multiple imaging modalities. *PLoS One* **2012,** *7* (12), e51314.

52. Andresen, M.; Stiel, A. C.; Trowitzsch, S.; Weber, G.; Eggeling, C.; Wahl, M. C.; Hell, S. W.; Jakobs, S., Structural basis for reversible photoswitching in Dronpa. *Proc. Natl. Acad. Sci. U. S. A.* **2007,** *104* (32), 13005-13009.

53. Adam, V.; Carpentier, P.; Violot, S.; Lelimousin, M.; Darnault, C.; Nienhaus, G. U.; Bourgeois, D., Structural basis of X-ray-induced transient photobleaching in a photoactivatable green fluorescent protein. *J Am Chem Soc* **2009,** *131* (50), 18063-18065.

54. Pletnev, S.; Subach, F. V.; Dauter, Z.; Wlodawer, A.; Verkhusha, V. V., A structural basis for reversible photoswitching of absorbance spectra in red fluorescent protein rsTagRFP. *J Mol Biol* **2012,** *417* (3), 144-151.

55. Testa, I.; D'Este, E.; Urban, N. T.; Balzarotti, F.; Hell, S. W., Dual channel RESOLFT nanoscopy by using fluorescent state kinetics. *Nano Lett* **2015,** *15* (1), 103-106.

56. Duwé, S.; Vandenberg, W.; Dedecker, P., Live-cell monochromatic dual-label sub-diffraction microscopy by mt-pcSOFI. *Chem Commun (Camb)* **2017,** *53* (53), 7242-7245.

57. Ganesan, S.; Ameer-Beg, S. M.; Ng, T. T.; Vojnovic, B.; Wouters, F. S., A dark yellow fluorescent protein (YFP)-based Resonance Energy-Accepting Chromoprotein (REACh) for Forster resonance energy transfer with GFP. *Proc. Natl. Acad. Sci. U. S. A.* **2006,** *103* (11), 4089-4094.

58. Murakoshi, H.; Shibata, A. C.; Nakahata, Y.; Nabekura, J., A dark green fluorescent protein as an acceptor for measurement of Forster resonance energy transfer. *Sci Rep* **2015,** *5*, 15334.

59. Murakoshi, H.; Shibata, A. C. E., ShadowY: a dark yellow fluorescent protein for FLIM-based FRET measurement. *Sci Rep* **2017,** *7* (1), 6791.

60. Pettikiriarachchi, A.; Gong, L.; Perugini, M. A.; Devenish, R. J.; Prescott,

M., Ultramarine, a chromoprotein acceptor for Forster resonance energy transfer. *PLoS One* **2012,** *7* (7), e41028.

61. Ando, R.; Mizuno, H.; Miyawaki, A., Regulated fast nucleocytoplasmic shuttling observed by reversible protein highlighting. *Science* **2004,** *306* (5700), 1370-1373.

62. Liu, Z.; Xing, D.; Su, Q. P.; Zhu, Y.; Zhang, J.; Kong, X.; Xue, B.; Wang, S.; Sun, H.; Tao, Y.; Sun, Y., Super-resolution imaging and tracking of protein-protein interactions in sub-diffraction cellular space. *Nat Commun* **2014,** *5*, 4443.

63. Hu, C. D.; Kerppola, T. K., Simultaneous visualization of multiple protein interactions in living cells using multicolor fluorescence complementation analysis. *Nat Biotechnol* **2003,** *21* (5), 539-545.

64. Lummer, M.; Humpert, F.; Wiedenlubbert, M.; Sauer, M.; Schuttpelz, M.; Staiger, D., A new set of reversibly photoswitchable fluorescent proteins for use in transgenic plants. *Mol Plant* **2013,** *6* (5), 1518-1530.

65. Testa, I.; Urban, N. T.; Jakobs, S.; Eggeling, C.; Willig, K. I.; Hell, S. W., Nanoscopy of living brain slices with low light levels. *Neuron* **2012,** *75* (6), 992-1000.

66. Schnorrenberg, S.; Grotjohann, T.; Vorbruggen, G.; Herzig, A.; Hell, S. W.; Jakobs, S., In vivo super-resolution RESOLFT microscopy of Drosophila melanogaster. *Elife* **2016,** *5:*e15567.

67. To, T. L.; Shu, X., Detecting Activity at Different Length Scales: From Subdiffraction to Whole-Animal Activity. *Biochemistry* **2017,** *56* (39), 5163-5164.

68. Klementieva, N. V.; Pavlikov, A. I.; Moiseev, A. A.; Bozhanova, N. G.; Mishina, N. M.; Lukyanov, S. A.; Zagaynova, E. V.; Lukyanov, K. A.; Mishin, A. S., Intrinsic blinking of red fluorescent proteins for super-resolution microscopy. *Chem Commun (Camb)* **2017,** *53* (5), 949-951.

69. Dickson, R. M.; Cubitt, A. B.; Tsien, R. Y.; Moerner, W. E., On/off blinking and switching behaviour of single molecules of green fluorescent protein. *Nature* **1997,** *388* (6640), 355-358.

70. Roebroek, T.; Duwé, S.; Vandenberg, W.; Dedecker, P., Reduced Fluorescent Protein Switching Fatigue by Binding-Induced Emissive State Stabilization. *Int J Mol Sci* **2017,** *18* (9).

71. Adam, V.; Berardozzi, R.; Byrdin, M.; Bourgeois, D., Phototransformable fluorescent proteins: Future challenges. *Curr Opin Chem Biol* **2014,** *20*, 92-102.

72. Dedecker, P.; De Schryver, F. C.; Hofkens, J., Fluorescent proteins: shine on, you crazy diamond. *J Am Chem Soc* **2013,** *135* (7), 2387-2402.

73. Chudakov, D. M.; Verkhusha, V. V.; Staroverov, D. B.; Souslova, E. A.; Lukyanov, S.; Lukyanov, K. A., Photoswitchable cyan fluorescent protein for protein tracking. *Nat Biotechnol* **2004,** *22* (11), 1435-1439.

74. Zhang, M.; Chang, H.; Zhang, Y.; Yu, J.; Wu, L.; Ji, W.; Chen, J.; Liu, B.; Lu, J.; Liu, Y.; Zhang, J.; Xu, P.; Xu, T., Rational design of true monomeric and bright photoactivatable fluorescent proteins. *Nat Methods* **2012,** *9* (7), 727-729.

75. Kim, J. H.; Lee, S. R.; Li, L. H.; Park, H. J.; Park, J. H.; Lee, K. Y.; Kim, M. K.; Shin, B. A.; Choi, S. Y., High cleavage efficiency of a 2A peptide derived from porcine teschovirus-1 in human cell lines, zebrafish and mice. *PLoS One* **2011,** *6* (4), e18556.

76. Lavoie-Cardinal, F.; Jensen, N. A.; Westphal, V.; Stiel, A. C.; Chmyrov, A.; Bierwagen, J.; Testa, I.; Jakobs, S.; Hell, S. W., Two-color RESOLFT nanoscopy with green and red fluorescent photochromic proteins. *Chemphyschem* **2014,** *15* (4), 655-663.

For TOC graph only: